Polarised Stimulated Emission Depletion Studies of Two-Photon Excited States

D. A. Armoogum, R. J. Marsh and A. J. Bain[+]

Department of Physics & Astronomy, University College London, Gower Street, London WC1E 6BT, UK

ABSTRACT

Stimulated emission depletion (STED) population and polarisation dynamics following two-photon excitation are investigated for rhodamine 6G in ethylene glycol. Time resolved fluorescence intensity and polarisation measurements were made using picosecond time-correlated single photon counting (TCSPC). Cross-sections for the stimulated transition were measured between 614nm (2.32×10^{-16} cm^2) and 663.5nm (6.05×10^{-17} cm^2), ground state vibrational lifetimes were found to vary between 314fs and 467fs. A collinear (180°) excitation-detection geometry was employed to investigate re-polarisation of the excited state array yielding fluorescence anisotropies above the two-photon limit. The circumvention of single-photon selection rules is demonstrated allowing the measurement of higher order parameters and correlation functions that are wholly inaccessible to 'conventional' (spontaneous) time resolved fluorescence techniques.

Key words: Stimulated emission depletion, vibrational relaxation, two-photon, polarisation, selection rules.

1. INTRODUCTION

Stimulated emission depletion (STED) of excited states has proved to be both a valuable tool in high resolution molecular spectroscopy[1], in time resolved spectroscopy as a means of orientational photoselection[2] and in the study of ultrafast vibrational relaxation within electronic ground states[3]. There has been considerable interest in the use of single-photon STED in fluorescence microscopy[4] where sub-wavelength image resolution has been recently demonstrated[5]. Recent work in our laboratory[6,7] has demonstrated the feasibility of performing STED in two-photon excited states. In this work femtosecond two-photon 800nm excitation (PUMP) of the widely used fluorescent probe fluorescein was followed by picosecond stimulated emission depletion (DUMP) of the excited state at 580nm. Time resolved detection was employed to determine changes in excited state population and alignment following STED together with the measurement of stimulated emission cross-sections and ground state vibrational relaxation times. In this paper stimulated emission cross-sections and ground state relaxation times for rhodamine 6G in ethylene glycol are determined from the (DUMP) energy dependence of the excited state depletion using a 90° excitation-detection geometry. We also investigate the polarisation dependence of two-photon STED using both parallel and orthogonal PUMP and DUMP polarisations and demonstrate excited state re-polarisation using a collinear excitation-detection geometry. Time resolved STED measurements can circumvent the constraints imposed by the selection rules for single-photon emission in that higher degrees of excited state order and correlation functions for molecular motion can be determined, measurements of hexadecapole alignment dynamics in rhodamine 6G are presented.

[+]Corresponding Author.

Proceedings of SPIE Vol. 5222 Nanocrystals, and Organic and Hybrid Nanomaterials, edited by David L. Andrews, Zeno Gaburro, Alexander N. Cartwright, Charles Y. C. Lee, (SPIE, Bellingham, WA, 2003) · 0277-786X/03/$15.00

2. POLARISED STIMULATED EMISSION DEPLETION

A schematic representation of the two-photon STED process in rhodamine 6G is shown in figure 1. Initial excitation from low lying vibrational levels in the S_0 ground state occurs via the simultaneous absorption of two (non resonant) near infra red photons with fast radiationless conversion yielding a vibrationally excited population in the S_1 excited electronic state. Fast collisional (and solvent) relaxation leads to the rapid population of lower vibrational levels in S_1. In the absence of external perturbations the population in S_1 decays by spontaneous emission to upper vibrational levels of S_0 followed by rapid collisional deactivation. In STED a visible laser pulse resonant with the $S_1 \rightarrow S_0$ emission is applied to induce transitions to upper vibrational levels of S_0. The net result of this process is a sharp reduction in the excited state population (fluorescence intensity) and a change in molecular alignment (fluorescence anisotropy) dependent on the relative polarisation of the two laser pulses. Depletion of the excited state is maximised for parallel PUMP and DUMP polarisations and at PUMP-DUMP delays that are short in comparison to the rotational diffusion time of the molecule[8,9]. STED dynamics can be modelled analytically in the limit of fast ground state relaxation and weak depletion of the excited state population. For strong saturation of the DUMP transition analytic solutions to the coupled rate equations (requiring numerical integration over the angular co-ordinates) are possible for model DUMP pulse shapes[6-7,9].

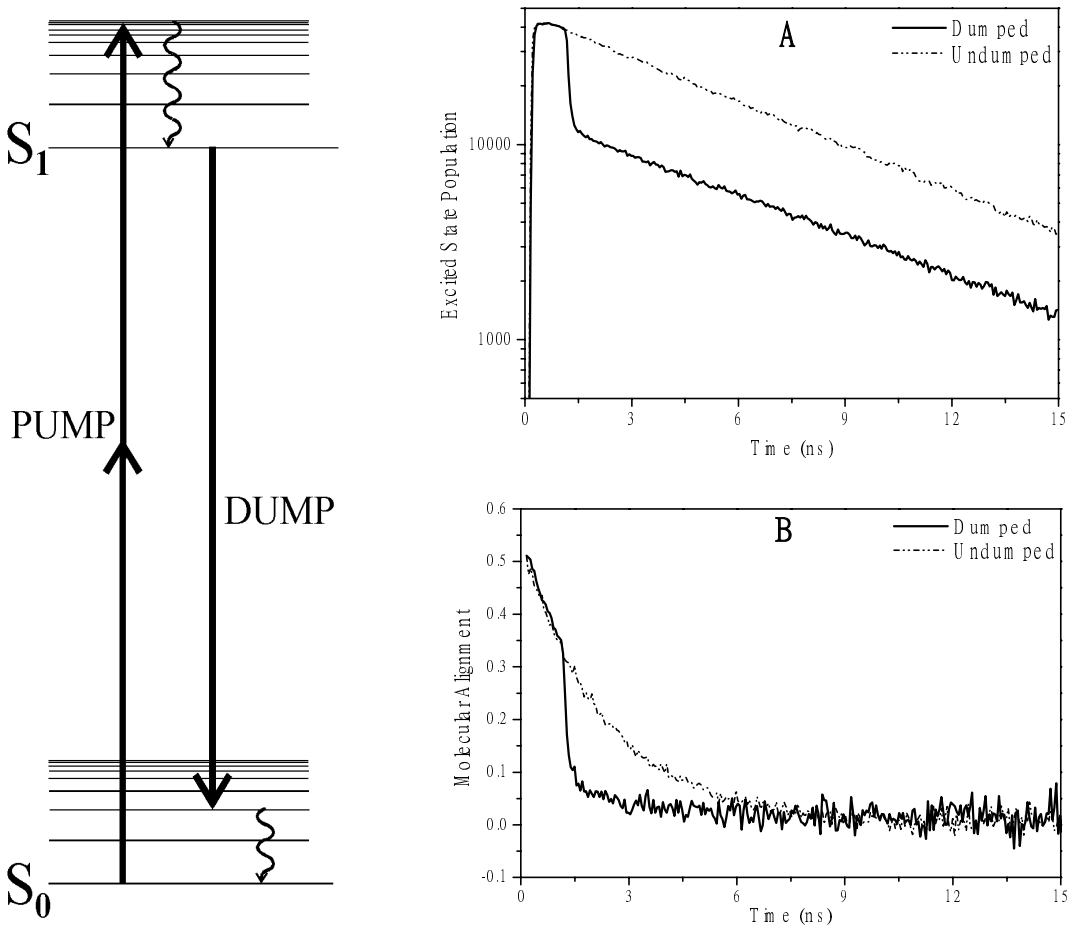

Figure 1: Stimulated emission depletion (STED) in rhodamine 6G. Linearly polarised two-photon excitation (PUMP) is followed by a time delayed (1ns) 17nJ, 622nm DUMP pulse. With parallel PUMP and DUMP polarisations both population (A) and alignment (B) reductions are maximised. The reductions in the excited state population and alignment are 70% and 0.23 respectively.

3. POPULATION AND ALIGNMENT CONTROL IN STED

3.1 Weak Depletion Analysis

The salient features of STED dynamics can be highlighted in the limit of weak excited state depletion and fast ground state relaxation. Here the analytic solution to the rate equations is particularly simple[7], the relationship between the initial (undumped) and final (dumped) orientational probability distribution functions being given by,

$$P_{ex}^{d}(\theta,\phi)=\frac{N_{ex}(u)}{N_{ex}(d)}P_{ex}^{u}(\theta,\phi)[1-SW_{D}(\theta,\phi)] \tag{1}$$

$P_{ex}^{u}(\theta,\phi)$ $N_{ex}(u)$ $N_{ex}(d)$ and $P_{ex}^{d}(\theta,\phi)$ are respectively the undumped (initial) and dumped (final) excited state populations and orientational distribution functions, $W_{D}(\theta,\phi)$ is the angular dependent DUMP transition probability and S is the saturation parameter for the transition given by

$$S=\sigma E/h\nu A \tag{2}$$

where σ is the stimulated emission cross-section, A is the beam area, E and hν are the dump pulse and photon energies respectively. Expressing the orientational distribution functions as spherical harmonic expansions[10] the moments of the altered distribution $\langle C_{KQ}^{ex}(d)\rangle$ are given by

$$\langle C_{KQ}^{ex}(d)\rangle=\frac{N_{ex}(u)}{N_{ex}(d)}\sum_{K'Q'}\langle C_{K'Q'}^{ex}(u)\rangle\langle KQ|1-SW_{D}(\theta,\phi)|K'Q'\rangle \tag{3}$$

3.2 Parallel PUMP and DUMP Polarisations: Excited State Depletion and Depolarisation

For parallel (Z) PUMP and DUMP polarisations (2) becomes

$$\langle C_{KQ}^{ex}(d)\rangle=\frac{N_{ex}(u)\sqrt{4\pi}}{3N_{ex}(d)}\sum_{K'Q'}\langle C_{K'Q'}^{ex}(u)\rangle\langle KQ|\left((3-S)Y_{00}(\theta,\phi)+\frac{2}{\sqrt{5}}SY_{20}(\theta,\phi)\right)K'Q'\rangle \tag{4}$$

Evaluation of the matrix elements for the observable moments of the altered array $\langle C_{00}^{ex}(d)\rangle$ and $\langle C_{20}^{ex}(d)\rangle$ [10] yields

$$\langle C_{00}^{ex}(d)\rangle=\frac{N_{ex}(u)}{3N_{ex}(d)}\left[(3-S)\langle C_{00}^{ex}(u)\rangle-\frac{2}{\sqrt{5}}S\langle C_{20}^{ex}(u)\rangle\right] \tag{5}$$

$$\frac{\langle C_{20}^{ex}(d)\rangle}{\sqrt{5}}=\frac{N_{ex}(u)}{3N_{ex}(d)}\left[(3-S)\frac{\langle C_{20}^{ex}(u)\rangle}{\sqrt{5}}-\frac{2}{5}S\langle C_{00}^{ex}(u)\rangle-\frac{4}{7}\frac{\langle C_{20}^{ex}(u)\rangle}{\sqrt{5}}+\frac{12}{35}\langle C_{40}^{ex}(u)\rangle\right] \tag{6}$$

From conservation of orientational probability $\langle C_{00}^{ex}\rangle$ is constant ($\sqrt{4\pi}$)[10]. The relationship between the initial and altered excited state populations is thus

$$N_{ex}(d)=\frac{N_{ex}(u)}{3}\left[(3-S)-\frac{2}{\sqrt{5}}S\langle\alpha_{20}^{ex}(u)\rangle\right] \tag{7}$$

Here $\langle\alpha_{20}^{ex}(u)\rangle$ is the normalised degree of excited state alignment[10] prior to excited state depletion. The fraction of the initial population remaining after application of the dump pulse is therefore,

$$F_{R}=\frac{N_{ex}(u)-N_{ex}(d)}{N_{ex}(u)}=1-\frac{S(1+2R(u))}{3} \tag{8}$$

The initial (undumped) fluorescence anisotropy R(u) is given by,

$$R(u)=\frac{\langle C_{20}^{ex}(u)\rangle}{\sqrt{5}\langle C_{20}^{ex}(u)\rangle}=\frac{\langle \alpha_{20}^{ex}(u)\rangle}{\sqrt{5}} \tag{9}$$

The fluorescence anisotropy immediately following stimulated depletion is, from (5) and (6),

$$R(d)=\frac{\left[\left(3-\frac{11}{7}S\right)R(u)-\frac{2}{5}S-\frac{12}{35}\langle \alpha_{40}^{ex}(u)\rangle S\right]}{(3-(1+2R(u))S)} \tag{10}$$

For two-photon excitation with a diagonal transition tensor the initial degrees of excited state K=2 and K=4 order are $4\sqrt{5}/7$ and $8/21$ respectively; for short PUMP-DUMP delays (8) and (10) become

$$\mathrm{F_R}=1-\frac{5}{7}\mathrm{S} \tag{11}$$

$$R(d)=\frac{4}{7}\left(1-\frac{5}{6}S\right)\Big/\left(1-\frac{5}{7}S\right) \tag{12}$$

3.3 Orthogonal PUMP and DUMP Polarisations: Excited State Depletion and Re-polarisation

Consider STED in which the angle β between the PUMP polarisation (Z) and that of the DUMP is varied between 0° and 90°. The PUMP and DUMP frames are connected by an Euler rotation D(0,β,0), in the PUMP axis system the angular dependence of the transition probability and the moments of the altered distribution are given by[8,9]

$$\langle C_{KQ}^{ex}(d)\rangle=\frac{N_{ex}(u)\sqrt{4\pi}}{3N_{ex}(d)}\sum_{K'Q'}\langle C_{K'Q'}^{ex}(u)\rangle\langle KQ\left|\left((3-S)Y_{00}(\theta,\phi)+\frac{2}{\sqrt{5}}S\sum_{q}d_{0q}^{2}(-\beta)Y_{2q}(\theta,\phi)\right)\right|K'Q'\rangle \tag{13}$$

where $d_{0q}^{2}(-\beta)$ are the reduced Euler rotation matrix elements for the transformation between the two axis systems. For β=90° (13) becomes

$$\langle C_{KQ}^{ex}(d)\rangle=\frac{N_{ex}(u)\sqrt{4\pi}}{3N_{ex}(d)}\sum_{K'Q'}\langle C_{K'Q'}^{ex}(u)\rangle\langle KQ\left|\begin{bmatrix}(3-S)Y_{00}(\theta,\phi)\\ -\frac{2S}{\sqrt{5}}\left[-\frac{1}{2}Y_{20}(\theta,\phi)+\sqrt{\frac{3}{8}}\left[Y_{22}(\theta,\phi)+Y_{2-2}(\theta,\phi)\right]\right]\end{bmatrix}\right|K'Q'\rangle \tag{14}$$

Evaluating matrix elements yields

$$\langle C_{00}^{ex}(d)\rangle=\frac{N_{ex}(u)}{3N_{ex}(d)}\langle C_{00}^{ex}(u)\rangle\left[(3-S)+\frac{1}{\sqrt{5}}S\langle \alpha_{20}^{ex}(u)\rangle\right] \tag{15}$$

$$\frac{\langle C_{20}^{ex}(d)\rangle}{\sqrt{5}}=\frac{N_{ex}(u)}{3N_{ex}(d)}\langle C_{00}^{ex}(u)\rangle\left[\left(3-\frac{5S}{7}\right)\frac{\langle \alpha_{20}^{ex}(u)\rangle}{\sqrt{5}}+\frac{S}{5}+\frac{6S}{35}\langle \alpha_{40}^{ex}(u)\rangle\right] \tag{16}$$

$$\frac{\left\{\langle C_{22}^{ex}(d)\rangle+\langle C_{2-2}^{ex}(d)\rangle\right\}}{\sqrt{30}}=-\frac{N_{ex}(u)}{3N_{ex}(d)}\langle C_{00}^{ex}(u)\rangle\frac{S}{5}\left[1-\frac{10\langle \alpha_{20}^{ex}(u)\rangle}{7\sqrt{5}}+\frac{\langle \alpha_{40}^{ex}(u)\rangle}{7}\right] \tag{17}$$

As the altered excited state is no longer cylindrically symmetric about Z the fluorescence intensity and polarisation will now depend on the cylindrically asymmetric degree of alignment written into the excited state by the DUMP pulse. The Z, X and Y components of the emission intensity following the application of the dump pulse are given by[9],

$$I_Z(d) = C\frac{N_{ex}(d)}{3}\left[1+\frac{2}{\sqrt{5}}\left\langle\alpha_{20}^{ex}(d)\right\rangle\right] \tag{18}$$

$$I_Y(d) = C\frac{N_{ex}(d)}{3}\left[1-\frac{1}{\sqrt{5}}\left\langle\alpha_{20}^{ex}(d)\right\rangle-\left(\frac{3}{10}\right)^{\frac{1}{2}}\left\{\left\langle\alpha_{22}^{ex}(d)\right\rangle+\left\langle\alpha_{2-2}^{ex}(d)\right\rangle\right\}\right] \tag{19}$$

$$I_X(d) = C\frac{N_{ex}(d)}{3}\left[1-\frac{1}{\sqrt{5}}\left\langle\alpha_{20}^{ex}(d)\right\rangle+\left(\frac{3}{10}\right)^{\frac{1}{2}}\left\{\left\langle\alpha_{22}^{ex}(d)\right\rangle+\left\langle\alpha_{2-2}^{ex}(d)\right\rangle\right\}\right] \tag{20}$$

where C is a constant of proportionality. With the loss of cylindrical symmetry the determination of excited state population changes requires the measurement of X, Y and Z polarisation components of the fluorescence intensity[10,11] and as a consequence both collinear and 90° excitation-detection geometries are necessary; this is in general impractical. Furthermore from (15) assuming a short PUMP-DUMP delay and an initial anisotropy of 4/7 the population remaining in the excited state is given by

$$\mathrm{F_R} = 1-\frac{\mathrm{S}}{7} \tag{21}$$

Comparison with (11) shows that population depletion is lower by a factor of five, in isotropic media this difference will become less marked as the excited state array relaxes. With initial (undumped) degrees of K=2 and K=4 alignment of 4/7 and 8/21 respectively a similar analysis to that above yields

$$\left\langle C_{00}^{ex}(d)\right\rangle = \frac{N_{ex}(u)}{3N_{ex}(d)}\left\langle C_{00}^{ex}(u)\right\rangle 3\left[\left(1-\frac{S}{7}\right)\right] \tag{22}$$

$$\frac{\left\langle C_{20}^{ex}(d)\right\rangle}{\sqrt{5}} = \frac{N_{ex}(u)}{3N_{ex}(d)}\left\langle C_{00}^{ex}(u)\right\rangle\frac{4}{7}\left[\left(3-\frac{S}{4}\right)\right] \tag{23}$$

$$\frac{\left\{\left\langle C_{22}^{ex}(d)\right\rangle+\left\langle C_{2-2}^{ex}(d)\right\rangle\right\}}{\sqrt{30}} = -\frac{N_{ex}(u)}{3N_{ex}(d)}\left\langle C_{00}^{ex}(u)\right\rangle\frac{S}{21} \tag{24}$$

In a medium with cylindrical asymmetry the measurement of the fluorescence anisotropy, defined (in a collinear excitation-detection geometry) by the Z and X polarisation components of the emission, is given by

$$R(d) = \left[\frac{\left\langle C_{20}^{ex}(d)\right\rangle}{\sqrt{5}}-\frac{\left\{\left\langle C_{22}^{ex}(d)\right\rangle+\left\langle C_{2-2}^{ex}(d)\right\rangle\right\}}{\sqrt{30}}\right]\Bigg/\left[\left\langle C_{00}^{ex}(d)\right\rangle+2\frac{\left\{\left\langle C_{22}^{ex}(d)\right\rangle+\left\langle C_{2-2}^{ex}(d)\right\rangle\right\}}{\sqrt{30}}\right] \tag{24}$$

The negative cylindrically asymmetric alignment contribution created by the DUMP pulse will act to increase the altered anisotropy, substitution of (21)-(23) into (24) yields

$$R(d) = \frac{4}{7}\left[\left(3-\frac{S}{6}\right)\right]\Bigg/\left[\left(3-\frac{11}{21}S\right)\right] \tag{25}$$

Re-polarisation of two-photon fluorescence above the maximum value of 4/7 should therefore in principle be possible provided the DUMP pulse is applied before there is significant orientational relaxation of the excited state population. As will be seen an increase in R(d) over R(u) of at least 10% is possible in rhodamine 6G yielding a fluorescence anisotropy in excess of the two-photon limit.

3.4 Circumventing Selection Rules: Measurement of Higher Order Parameters and Hidden Correlation Functions

All fluorescence experiments irrespective of the nature of the excitation process (i.e. single or multiphoton) are restricted in the information that can be obtained on excited state dynamics and order. The selection rules for spontaneous electric dipole emission restricts the contribution of $P_{ex}(\theta,\phi)$ to moments of rank K=0 (population) and K=2 (alignment)[11,13]. As a result the time resolved fluorescence anisotropy is determined solely by second order dipole correlation functions. In isotropic media under specific conditions (e.g. small step rotational diffusion the measurement of one correlation function (i.e. that for K=2) is sufficient to determine the full angular motion of a molecular probe. We have recently shown that in ordered media these simple considerations no longer hold[10,12-15], there are significant contributions to the molecular distribution function from higher order moments. The measurement of higher order correlation functions for molecular motion is therefore essential. Time resolved STED allows these issues to be addressed, with parallel PUMP and DUMP polarisations the undumped and dumped anisotropies are related through (14),

$$R(d)=\frac{\left[\left(3-\frac{11}{7}S\right)R(u)-\frac{2}{5}S-\frac{12}{35}\left\langle\alpha_{40}^{ex}(u)\right\rangle S\right]}{\left(3-(1+2R(u))S\right)} \tag{26}$$

Measurement of R(d), R(u) and S (via F_R) as a function of the PUMP-DUMP delay allows the time evolution of $\left\langle\alpha_{40}^{ex}\right\rangle$ to be determined from (26). The validity of this approach can be tested by measurement of the relaxation dynamics of $\left\langle\alpha_{40}^{ex}(t)\right\rangle$ created by two-photon excitation of rhodamine 6G in ethylene glycol. Here orientational relaxation dynamics are well described by small step rotational diffusion[10] in which the alignment relaxation times (τ_{KQ}) are given by

$$\tau_{KQ}=\left(DK(K+1)\right)^{-1} \tag{27}$$

The relationship between the directly measurable fluorescence anisotropy decay time (τ_{20}) and that for $\left\langle\alpha_{40}^{ex}\right\rangle$ is therefore

$$\tau_{40}=0.3\tau_{20} \tag{28}$$

Determination of τ_{40} for rhodamine 6G in ethylene glycol is discussed below.

4. EXPERIMENTAL PROCEDURE

The experimental apparatus for STED is illustrated in figure 2. The sample, a $5\text{x}10^{-4}$M solution of rhodamine 6G (Coherent) in ethylene glycol was contained in a 1cm quartz cuvette (Hellma) with four optical windows. Two-photon excitation was achieved using the partial output of a regeneratively amplified Ti:Sapphire laser (Coherent Mira 900F, Coherent RegA 9000) which provided 800nm laser pulses with up to 60nJ energy and 140fs FWHM pulse width at a repetition rate of 250kHz. The majority of the 800nm output (ca. 3.4μJ) was used to pump an optical parametric amplifier (Coherent OPA 9400) which provides a synchronous (ca. 250fs) pulse train tuneable across the visible spectrum (450-700nm). To prevent saturation at low dump energies (ca. 1nJ) and DUMP induced two-photon fluorescence, the OPA pulses were stretched to ca. 900fs using the material dispersion provided by passage through a distilled water cell. The PUMP and DUMP wavelengths were measured using a laser spectrum analyser (IST-Rees), and the pulse widths monitored using a scanning autocorrellator (APE). PUMP and DUMP beam polarisations were controlled using broadband half waveplates and cube polarisers (Melles-Griot). The PUMP-DUMP separation could be set and scanned using a variable optical delay line (Time & Precision). PUMP and DUMP powers were controlled by neutral density wheels and measured by a precision power meter (Anritsu). Prior to the experimental sample the PUMP and DUMP beams were spatially overlapped using a broadband dichroic beam combiner (CVI Optics). For effective two-photon STED, it is necessary to select DUMP wavelengths within the emission region of the fluorescent molecule for which there is a low cross-section for single and two-photon absorption. Rhodamine 6G has a broad emission spectrum with detectable fluorescence spanning ca. 540-700nm. The emission peak in ethylene glycol was measured at 552nm, however there is still considerable single-photon absorption at this wavelength (ca. 16% of the extinction at the

530nm absorption maximum[16]). Rhodamine 6G also possesses a significant two-photon absorption cross-section at wavelengths close to the near infra-red (ca. 1.5×10^{-48} ($cm^4 s$)/photon at 700nm[17]). To minimise the effects of single- and two-photon background fluorescence, the DUMP pulse is therefore restricted to a region between these two extremes. A DUMP wavelength range of 614nm to 663.5nm was chosen; at 614nm the fluorescence intensity is 28% of the peak at 552nm, but the single-photon extinction coefficient at this wavelength is less than 0.1% of the maximum value.

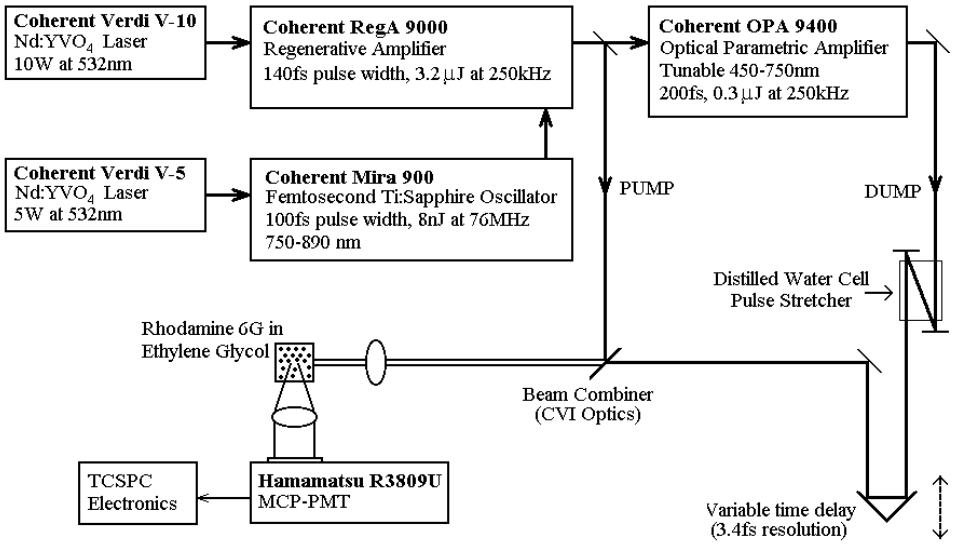

Figure 2: Schematic diagram of the femtosecond laser system and 90° excitation-detection geometry used in the STED experiments. Group velocity dispersion from a distilled water cell is used to stretch the DUMP pulses from 200fs to ca. 900fs thus reducing both the saturation of the DUMP transition and background signal caused by secondary two-photon excitation. A collinear (180°) excitation-detection geometry is employed for re-polarisation experiments (see figure 3).

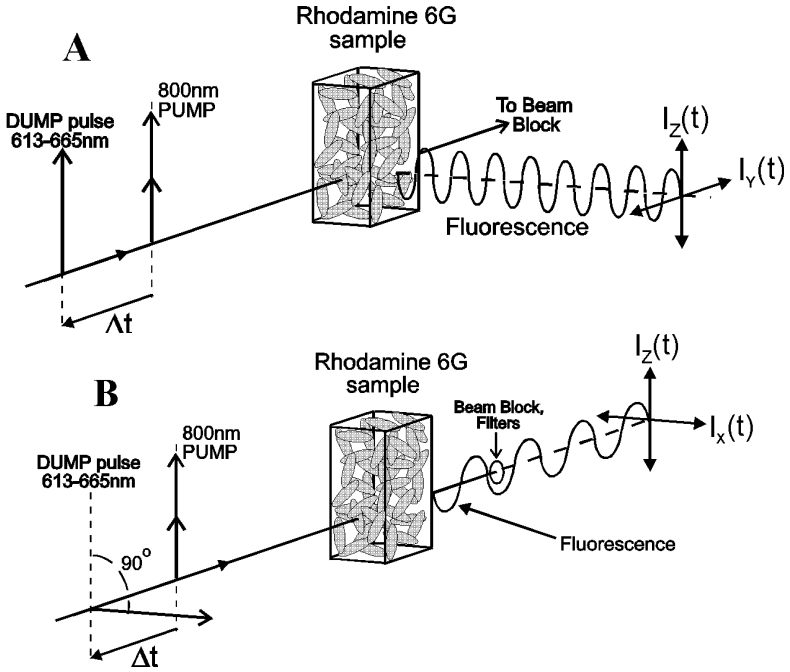

Figure 3: Excitation-detection geometries employed in the time resolved stimulated emission depletion experiments. (A) Measurements of ground state vibrational lifetimes, stimulated emission cross-sections and excited state hexadecapolar order evolution for rhodamine 6G used a parallel "V-V" PUMP-DUMP configuration with fluorescence detected at 90°. (B) Re-polarisation of the rhodamine 6G excited state employed a "V-H" PUMP-DUMP collinear geometry.

4.1 Measurement of stimulated emission cross-sections and ground state relaxation times

Determination of the stimulated emission cross-sections and ground state relaxation times over the DUMP wavelength range was carried out using the conventional 90° excitation-detection geometry (figure 3A), scattered laser light was blocked using an interference filter (Corion LS600) and glass cut-off filters (Schott BG39). A glass cut-off filter (Schott OG590) was placed in the DUMP path before the sample to block short-wavelength remnants of white continuum generated in the OPA. A 300μm slit was used to isolate the waist region of the beams. Time resolved fluorescence lifetime and anisotropy measurements at fixed PUMP-DUMP delays were performed using picosecond photon counting[7,13]. Excited state population depletion measurements were obtained from dumped and undumped total fluorescence intensity decays $[I_Z(t)+2I_Y(t)]$. Fine adjustments to the PUMP and DUMP energies were made using neutral density wheels (Melles-Griot). The typical on-sample PUMP pulse energies were below 30nJ; the DUMP pulse energy was varied between 0 and 33nJ.

4.2 Excited State Re-polarisation

To achieve re-polarisation of the excited state fluorescence anisotropy a collinear (180°) excitation-detection geometry was employed together with crossed PUMP and DUMP polarisations (figure 3B). The collinear geometry of the experiment required more aggressive filtering of the PUMP and DUMP pulses (16nJ at 800nm and 12.5nJ at 614nm respectively). To this end several short pass interference filters (Corion LS550, 2xCoherent Short-pass COWL 580nm, 2xCoherent Short-pass COWL 540nm) were used in conjunction with a beam block to avoid laser breakthrough.

4.3 Measurement of K=4 Dynamics

Measurement of $\langle \alpha_{40}^{ex}(t) \rangle$ dynamics was undertaken using fluorescence intensity and depolarisation measurements in the 90° excitation–detection geometry as employed for the determination of stimulated emission cross-sections and ground state relaxation times. A DUMP wavelength of 640nm was chosen and the PUMP-DUMP delay was varied between 150ps and 1500ps for constant on-sample PUMP and DUMP powers (28nJ and 4nJ respectively).

5. RESULTS

5.1 Stimulated Emission Dynamics in Rhodamine 6G

Measurements of the degree of excited state depletion as a function of DUMP pulse energy were undertaken at wavelengths spanning 614 and 663.5nm with autocorrelation widths between 1.2ps and 1.32ps (848fs-933fs assuming Gaussian pulse shapes). PUMP-DUMP delays of 650ps-1ns were used such that the effects of solvent and excited state relaxation could be neglected. The results together with fits to the data using numerical solutions to the coupled rate equations[7,9] are shown in figure 4. All five data sets show a characteristic energy dependence with an initial low-energy linear regime with the onset of saturation at higher dump energies corresponding to re-pumping of the excited state due to the finite lifetime of the target vibrational levels in the ground state. Values obtained for the stimulated emission cross-sections and ground state vibrational relaxation times are shown in table 1. The values of the stimulated emission cross-sections (essentially obtainable from the linear portions of the DUMP depletion data) show a steady decrease with increasing DUMP wavelength from 2.32×10^{-16}cm^2 (614nm) to 6.1×10^{-17}cm^2 (663.5nm) consistent with the relative intensities of fluorescence at these wavelengths. Ground state vibrational relaxation times (reflected in the nonlinear energy dependence) were found to vary between 467fs and 314fs. Increasing the DUMP wavelength gives rise to the population of higher lying vibrational levels within S_0 over 614nm to 663.5nm; the increase in ground state vibrational energy is approximately 1200cm^{-1} compared to a thermal energy of ca. 200cm^{-1}. Between 614nm and 644.5nm the stimulated emission cross-sections are of sufficient magnitude to allow coverage of the nonlinear depletion region; at 663.5nm DUMP pulse energies in excess of 35nJ are required to achieve comparable data sets. Up to 644nm there is an apparent decrease in the ground state relaxation time of ca.100fs with an increase in vibrational energy of ca. 770 cm^{-1} (table 1).

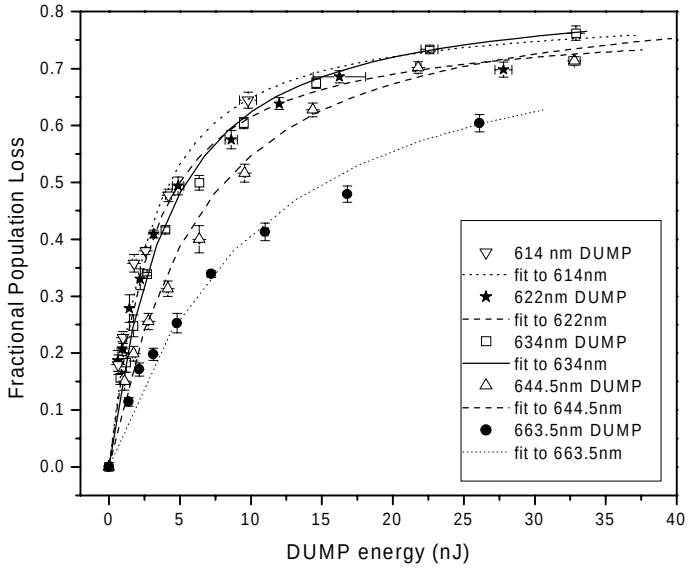

Figure 4: Excited state population loss for rhodamine 6G in ethylene glycol as a function of DUMP energy for wavelengths between 614 and 663.5nm. Fits to experimental data using solutions of the coupled rate equations are shown (solid and dashed lines) and yield stimulated emission cross-sections and ground state vibrational relaxation lifetimes for the five transitions (see table 1).

DUMP Wavelength (nm)	Stimulated Emission Cross-Section (10^{-16}cm^2)	Ground State Vibrational Relaxation Lifetime (fs)	Excess Vibrational Energy Relative to 614nm (cm^{-1})
614	2.32	424	0
622	2.26	445	209
634	1.65	365	514
644.5	1.07	314	771
663.5	0.61	467	1215

Table 1: Values of the stimulated emission cross-sections and ground state vibrational relaxation times obtained from fits to the depletion data of figure 4. The final column shows the relative energy of the target vibrational levels in the ground state relative to those populated at 614nm.

5.2 Excited State Re-polarisation

Figure 5 shows the results following implementation of the collinear STED arrangement to permit re-polarisation of two-photon excited fluorescence in rhodamine 6G. A short PUMP-DUMP delay of 6ps was employed to negate the effects of excited state alignment relaxation (K=2 and K=4) due to rotational diffusion (τ_{20}=1.74ns). Two-photon excitation (undumped) in rhodamine 6G yields an initial fluorescence anisotropy of 0.508; this differs from the predicted value of 0.571 by a factor ($\bar{A}$) of 0.889, this is similar to the deviation measured for single photon excitation relative to the theoretical limit of 2/5[10]. Application of the DUMP pulse yields an initial anisotropy of 0.615, an increase of 10% and well above the 0.571 limit. Reduction in initial fluorescence anisotropy values from theory can arise from differences in absorption and emission transition dipole moment directions, an instrument response time comparable with the rotational relaxation time (not an issue here) and de-polarisation arising from optical components[13]. With $\bar{A}$=1, the re-polarised anisotropy would be close to 0.7 (see table 2).

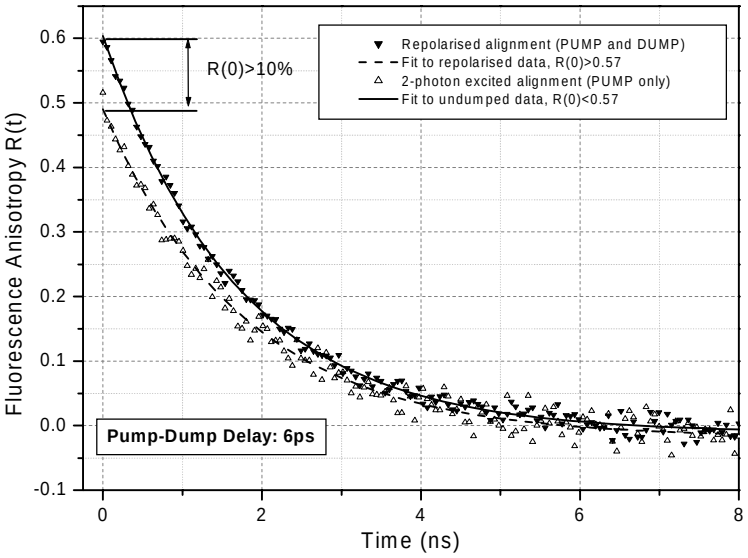

Figure 5: Excitation and re-polarisation of the rhodamine 6G molecular alignment by perpendicular PUMP and DUMP fields. Introduction of a horizontally polarised DUMP field 6ps after excitation modifies the excited state alignment to a value above the two-photon limit.

Dataset	$R(0)_{uncorrected}$	$\bar{A}$	$R(0)_{corrected}$	*2 photon limit=0.571*
PUMP only	0.508	0.889	0.571	*3 photon limit=0.667*
PUMP-DUMP	0.615	0.889	0.692	*4 photon limit=0.727*

Table 2: Values of the initial (time zero) fluorescence anisotropy obtained for two-photon excitation of rhodamine 6G with and without the presence of a strong horizontally polarised DUMP pulse. A further correction of the anisotropy (due to experimental and/or molecular factors) indicates that under ideal conditions an initial anisotropy value of 0.692 would be obtained, which lies between the three- and four-photon excitation limits.

5.3 K=4 Rotational Diffusion Dynamics

Figure 6 shows a plot of the values of $\langle \alpha_{40}^{ex}(t) \rangle$ obtained from population and anisotropy measurements using (10) for a series of PUMP-DUMP delays from 150ps to 1.5ns. Rotational diffusion of rhodamine 6G in ethylene glycol is well described by small-step rotational diffusion yielding a single exponential decay of the (undumped) fluorescence anisotropy of 1.74ns. A single exponential fit to the data in figure 6 yields a relaxation time of 480ps, close to the τ_{40} relaxation time of 522ps predicted by direct measurement of τ_{20}. It should be noted that the analytical model used to extract values of $\langle \alpha_{40}^{ex}(t) \rangle$ (10) is only valid in the limit of weak excited state depletion and fast ground state relaxation. However, modelling of STED dynamics using solutions to the population rate equations[7] indicates that outside the weak depletion limit this approach, although yielding (a correctable) offset in the magnitude of $\langle \alpha_{40}^{ex}(t) \rangle$, has little effect on the measured decay[18].

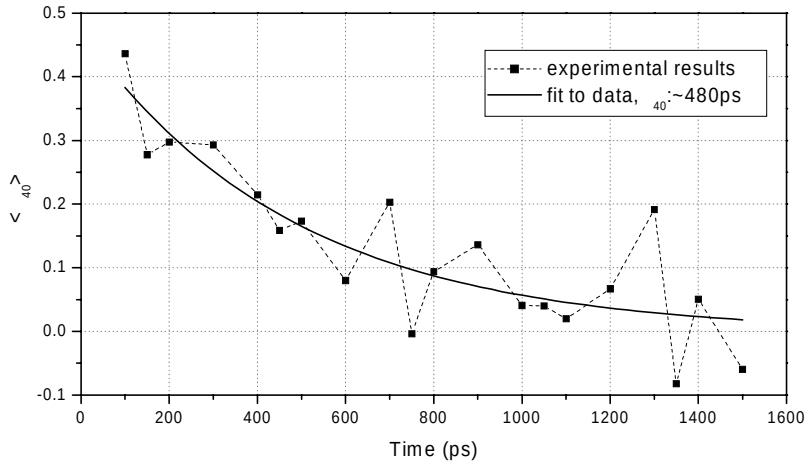

Figure 6: A plot of the evolution of the K=4 (hexadecapole) excited state moment for rhodamine 6G in ethylene glycol. An exponential fit yielding τ_{40}=480ps compares favourably with the theoretical value of 522ps.

6. CONCLUSIONS

Two-photon STED has been successfully demonstrated in rhodamine 6G over a range of wavelengths (614-663.5nm). Time resolved PUMP-DUMP lifetime and anisotropy measurements have shown that precise population and orientation control of the excited state array is possible. Moreover we have demonstrated that STED is capable of breaking single-photon selection rules allowing access to hitherto hidden information on molecular structure, dynamics and geometry.

ACKNOWLEDGEMENTS

We would like to thank EPSRC and the UCL Graduate School for support of this work.

REFERENCES

[1] D E Reisner, R W Field, J L Kinsey and H-L Dai, J. Chem. Phys. **80**, 5968-5978 (1984)
[2] I Gryczynski, J Kusba and J R Lackowicz, J. Phys. Chem. US **98**, 8886-8895 (1994), J Kusba, V Bogdanov, I Gryczynski and J R Lackowicz, Biophys. J. **67**, 2024-2040 (1994)
[3] S A Kovalenko, J Ruthmann and N P Ernsting, J. Chem. Phys. **109**, 1894-1900 (1998)
[4] C Buehler, C Y Dong, P T C So, T French and E Gratton, Biophys. J. **79**, 536-549, (2000)
[5] T A Klar, S Jakobs, M Dyba, A Egner and S W Hell, Proc Nat Acad Sci (USA) **97**, 8206-8210 (2000)
[6] D A Armoogum, A J Bain and R J Marsh, Proc. SPIE **4812**, 45-54 (2002)
[7] R J Marsh, D A Armoogum and A J Bain, Chem. Phys. Lett. **366**, 398-405 (2002)
[8] A J Bain, R J Marsh and D A Armoogum , UK patent application 0211781.0. (22nd May 2002)
[9] A J Bain, R J Marsh and D A Armoogum (to be published)
[10] A J Bain, P Chandna, and J Bryant, J. Chem. Phys. **112**, 10418-10434 (2000)
[11] A J Bain and A J McCaffery, J. Chem. Phys. **83**, 2641-2645 (1984)
[12] A J Bain in *An Introduction to Laser Spectroscopy*, (D L Andrews and A Demidov, eds.) pp 171-210, Kluwer Scientific, London (2002)
[13] A J Bain, P Chandna, G Butcher and J Bryant, J. Chem. Phys. **112**, 10435-10449 (2000)
[14] D A Armoogum, J Bryant, E M Monge and A J Bain, Proc. SPIE **4799**, 63-73 (2002)
[15] E M Monge, D A Armoogum and A J Bain, Proc. SPIE **4797**, 264-274 (2002)
[16] U Brackmann, *LambdaChrome® Laser Dyes* (3rd Ed.), Lambda Physik AG, Goettingen (2000)
[17] M A Albota, C Xu and W W Webb, *Applied Optics* **37**(31), 7352-7356 (1998)
[18] R J Marsh, D A Armoogum and A J Bain (to be published)